Chaos, Solitons & Fractals Vol. 2, No. 4, pp. 377–392, 1992
Printed in Great Britain

0960-0779/92$5.00 + .00

Compact Billiards in Phase Space

A. M. OZORIO DE ALMEIDA*

Instituto de Matemática Pura e Aplicade, Estrada Dona Castorina 110, 22460, Rio de Janeiro, RJ, Brazil

and

M. A. M. DE AGUIAR

Departamento de Física do Estado Sólido e Ciêoncia de Materiais, Instituto de Física, Universidade Estadual de Campinas, 13081 – Campinas, SP, Brazil

(*Received* 23 *April* 1992)

Abstract—Compact billiards in phase space, or action billiards, are defined by truncating the classical Hamiltonian in the action variables. The corresponding quantum mechanical system has a finite Hamiltonian matrix. In this paper we define the compact analogue of common billiards, i.e. straight motion in phase space followed by specular reflections at the boundaries. Computation of their quantum energy spectra establishes that their properties are exactly those of regular billiards: the short range statistics follow the known universality classes depending on the regular or chaotic nature of the motion, whereas the long range fluctuations are determined by the periodic orbits.

1. INTRODUCTION

Motion in a square well illustrates many of the important features of wave mechanics, though the corresponding classical problem is ignored in elementary texts. In two or more dimensions, however, the corresponding billiard problem illuminates important features of both classical and quantum mechanics. This is because the motion inside the billiard is trivial, so that the regular or chaotic profile of the classical motion and its quantum effects depend exclusively on the shape of the billiard boundary.

In spite of this vast simplification, it must be noted that the billiard is bounded only in its position coordinates. In contrast the momenta suffer no restrictions, so that the accessible phase space is unbounded. As a consequence the Hilbert space spanned by the eigenstates of the quantum billiard is also infinite, which implies the practical need to truncate any basis used to calculate energy eigenvalues or eigenstates. This is especially distressing in studies of the semiclassical limit, where the need to use an ever growing basis arises in an uncontrolled way.

This difficulty has stimulated interest in the study of the quantization of maps defined on compact phase spaces [1–3]. A novel approach was proposed by the authors of Ref. [4] where instead of compactifying the phase space we can effectively limit the motion to a compact domain by introducing cut-offs to the classical Hamiltonian, thus creating an 'Action Billiard'. The corresponding quantum mechanical effect was shown to be precisely

*Permanent address: Instituto de Física, UNICAMP, Campinas, 13081, SP, Brazil.

the truncation of the Hamiltonian matrix in the harmonic oscillator representation that one would perform in a practical calculation.

As first envisaged action billiards were applied [4, 5] to problems where the cut-off did not perturb much of the classical motion. In this they contrasted with normal billiards where the boundaries inevitably break the free unperturbed motion. The purpose of this paper is to present new forms of billiards that have identical properties to normal billiards, that is, straight motion in phase space followed by specular deflections at the boundaries, though the phase space motion is bounded. These are action billiards as defined in [4] so that the free motion is in action with the angle kept constant. Though this appears unnatural, we show in Section 2 that it can be interpreted as a distortion of ordinary motion in a square well, to which it tends smoothly in the limit of small energies. The Hamiltonian operator corresponding to the action billiard is discussed in Section 3, where we derive the smoothed 'Weyl term' of the energy level density. Section 4 is devoted to numerical results for various features of the level density fluctuations. In Section 5 we discuss the way in which this entirely novel quantization of billiards confirms existing hypotheses and theories connecting the chaotic or regular character of the classical motion to the spectral statistics of the quantized system.

2. COMPACT BILLIARDS

A particle in a one-dimensional box has the free Hamiltonian

$$H(p, q) = p^2/2 \tag{2.1}$$

inside the box, so that between collisions with the hard walls the momentum remains fixed at $p = \pm \sqrt{(2E)}$ where E is the constant energy. For fixed energy the motion remains bounded in phase space as the momentum switches periodically between its allowed values at each collision. However, the allowed region of phase irrespective of energy is the infinite strip shown in Fig. 1(a).

One way to compactify this region is to consider the vertical lines intersecting the horizontal axis at q_1 and q_2 to be approximations to concentric circles centred on the q axis. The further the centre is the from q_1 and q_2, the larger will be the region where this

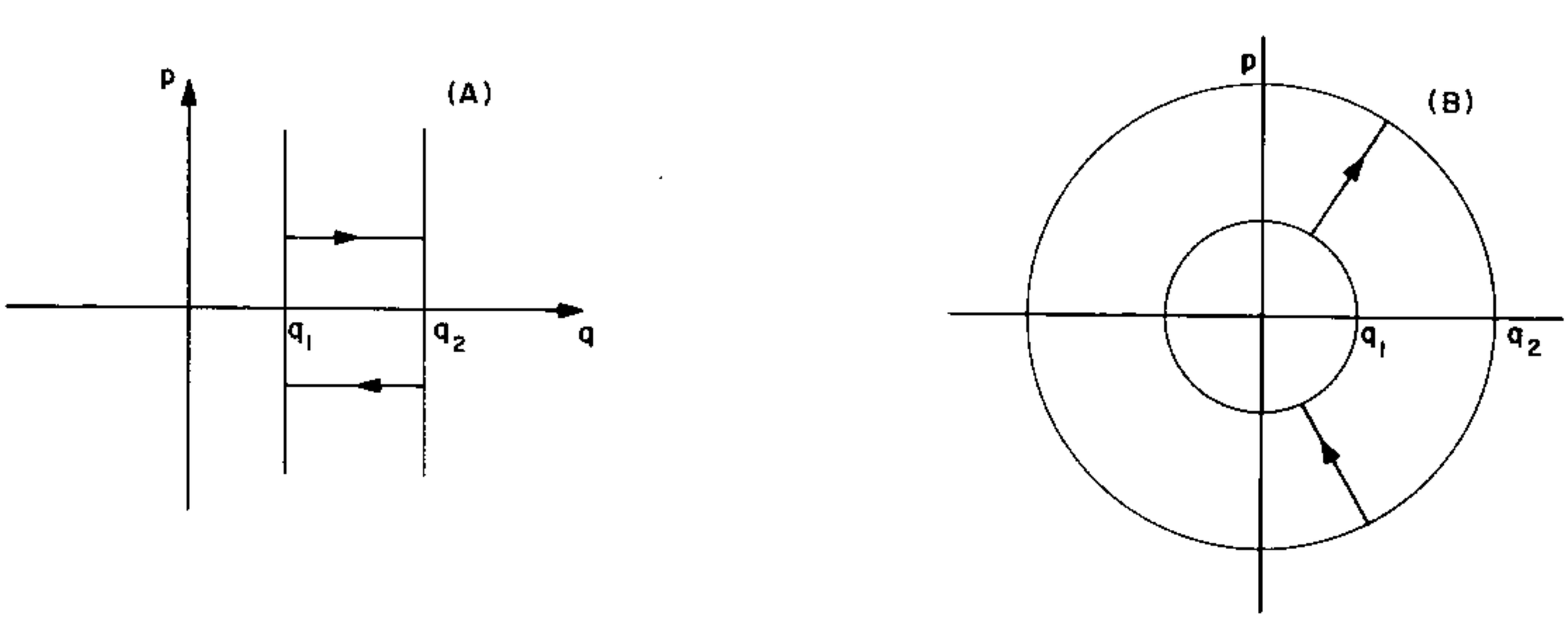

Fig. 1. (a) Ordinary one-dimensional billiard with walls at q_1 and q_2; (b) compactification of phase space generating the action billiard.

approximation holds. The advantage of this view is that now the annular region bounded by the two circles is finite. Placing the centre at the origin and switching to canonical polar coordinates in phase space (i.e. the action-angle variables of the harmonic oscillator):

$$p^2 + q^2 = 2I, \qquad p/q = \tan\theta, \tag{2.2}$$

we obtain the simple equation $I = q_1^2/2 = \mathcal{J}_1$ and $I = q_2^2/2 = \mathcal{J}_2$ for the boundary circles.

All that remains is to choose the Hamiltonian for this compactified square well. For small E the free Hamiltonian (2.1) is quite satisfactory, but for $E > q_1^2/2$ the character of the motion changes completely. It is therefore better to use the fact that in the action-angle variables the motion in the compactified well [Fig. 1(b)] will look just like that of the ordinary well if we choose the Hamiltonian as an even function of θ. The simplest choice is

$$H(I, \theta) = -\cos\theta, \tag{2.3}$$

so that we obtain straight radial motion between the circles that is reversed at every collision, as shown in Fig. 1(b). For small energies, we have

$$H(I, \theta) \simeq -1 + \theta^2/2, \tag{2.4}$$

so that we recover the usual motion in a box by approximating the radial motion by that along horizontal lines.

The generalization for two-dimensional billiards is now immediately

$$H(\theta_1, \theta_2) = -\cos\theta_1 - \cos\theta_2 \tag{2.5}$$

within its walls. These are functions only of the actions:

$$F(I_1, I_2) = \text{constant}. \tag{2.6}$$

Since the one-dimensional motion for the compactified box is the same in polar (I, θ) coordinates as that for the original box in (p, q) coordinates, we obtain the same law for the specular reflection of orbits at the boundary, that is, the angle of reflection must equal the angle of incidence.

The validity of the present billiard problem can be ascertained by considering the sharp collisions with the boundary to be the limit of smooth Hamiltonians. This was in fact the procedure followed in [4]. The present billiards fit perfectly into the general class of action billiards treated there. Hence we will be able to use the previous treatment for quantizing these new action billiards, even though the Hamiltonian has an unusual form. The advantage is that now we can treat billiards whose classical motion is well known. In this paper we shall consider square and circular billiards, which are known to be integrable, as well as the chaotic Bunimovich billiard or stadium.

3. QUANTIZATION

The general rule deduced in [4] for calculating the Hamiltonian matrix of a general action billiard is first to calculate the matrix elements of the free Hamiltonian (without billiard walls) in the harmonic oscillator representation. In the present case, the simplest choice is to start from

$$\cos\theta = \frac{q}{\sqrt{(q^2 + p^2)}}. \tag{3.1}$$

Using step operators a and a^+ we have

$$\hat{q} = \frac{a + a^+}{\sqrt{2}}, \tag{3.2}$$

so we then obain for each degree of freedom

$$\hat{H} = \frac{1}{\sqrt{2}} [a(a^+a + aa^+)^{-1/2} + (a^+a^+ + aa^+)^{-1/2}a^+]. \tag{3.3}$$

In the one dimensional case, this corresponds to a tridiagonal Hamiltonian matrix with zero elements at the diagonal. As a consequence the trace is zero. Since the spectrum of $\cos\theta$ is the same as that of $-\cos\theta$, the eigenvalues come in symmetry pairs. One may worry over the singular nature of this Hamiltonian, but in the harmonic oscillator representation, to which we shall keep, we simply have

$$(a^+a + aa^+)^{-1/2}|n\rangle = [(n + \tfrac{1}{2})\hbar]^{-1/2}|n\rangle. \tag{3.4}$$

The limitation of the classical phase space now manifests itself in the fact that only the states $|n_1 n_2\rangle$, such that $I_1 = (n_1 + \frac{1}{2})\hbar$ and $I_2 = (n_2 + \frac{1}{2})\hbar$ lie inside the billiard, are to be kept in the expansion of the Hamiltonian. The billiard boundary uncouples these states from all the others so that the basis is finite. In the semiclassical limit, $\hbar \to 0$, the number of states participating grows without bound, but the size of the Hamiltonian matrix is finite for each non-zero $\hbar$.

Once the spectrum has been obtained we shall be interested in its statistical properties. Besides the nearest neighbour distribution (NND), the density of states

$$\eta(E) = \sum_n \delta(E - E_n)$$

is of great interest. According to Gutzwiller [6], in the semiclassical limit this can be separated into a smooth term, called the Weyl term, plus a series of oscillatory quantum corrections due to periodic orbits:

$$\eta(E) \simeq n_{\text{Weyl}} + n_{\text{osc}}$$

where

$$n_{\text{Weyl}} = \frac{1}{h^2} \int \delta(H - E)\,\mathrm{d}V, \tag{3.5}$$

$$n_{\text{osc}} = \sum_{\text{p.o.}} A_{\text{p.o.}} \mathrm{e}^{iS/\hbar + \text{phases}}$$

and $A_{\text{p.o.}}$ are weights depending on the stability and period of each periodic orbit.

Before getting to numerical results let us first calculate the Weyl term analytically for the Hamiltonian (2.5). We start with the smooth step function

$$N(E) = \frac{1}{h^2} \int \Theta(H - E)\,\mathrm{d}V = \frac{1}{h^2} \int_{H \leqslant E} \mathrm{d}V \tag{3.6}$$

and then calculate

$$\eta_{\text{Weyl}}(E) = \frac{\mathrm{d}N}{\mathrm{d}E}.$$

If $\mathscr{A}$ is the area enclosed by the billiard, then

$$N(E) = \frac{\mathscr{A}}{h^2} \int \mathrm{d}\theta_1 \mathrm{d}\theta_2.$$

For $-2 < E < 0$, it is easy to check that

$$N(E) = \frac{4\mathcal{A}}{h^2}\int_0^a \theta_2 \mathrm{d}\theta_1 = \frac{4\mathcal{A}}{h^2}\int_0^a \text{arc cos}\,(-E - \cos\theta_1)\mathrm{d}\theta_1$$

where

$$\cos a = -E - 1. \tag{3.7}$$

Differentiating with respect to E and using (3.7) we get

$$n_{\text{Weyl}} = \frac{4\mathcal{A}}{h^2}\int_0^a \frac{\mathrm{d}\theta_1}{\sqrt{[1 - (-E - \cos\theta)^2]}}$$

which, in terms of the new variable

$$y = \cos\omega_1 + E/2$$

simplifies to

$$n_{\text{Weyl}} = \frac{8\mathcal{A}}{h^2}\int_0^a \frac{\mathrm{d}y}{\sqrt{R(y)}} \tag{3.8}$$

where

$$R(y) = (y^2 - a_-^2)(y^2 - a_+^2),$$
$$a_\pm^2 = (1 \mp E/2)^2.$$

Expression (3.8) can be identified as a complete elliptic integral of the first kind [7]:

$$n_{\text{Weyl}} = \frac{8\mathcal{A}}{h^2 a_+} F(\pi/2,\, a_-/a_+) \tag{3.9}$$

where

$$F(\pi/2,\, K) = \int_0^{\pi/2} \frac{\mathrm{d}\theta}{\sqrt{(1 - K^2\sin^2\theta)}}.$$

It is easy to check that $\eta_{\text{Weyl}}(E) = \eta_{\text{Weyl}}(-E)$ and that $n_{\text{Weyl}}(0) = \infty$.

Remembering that n_{Weyl} is constant for common two-dimensional billiards we see that the price to be paid for the unusual Hamiltonian (2.5) is a much more complicated expression for the Weyl density. Nevertheless, equation (3.9) still gives a closed form for n_{Weyl} and we shall discuss this formula in the next section in connection with the numerical results.

4. NUMERICAL RESULTS

The billiard geometries considered in this paper are displayed in Fig. 2. The dimension of these billiards will be kept constant throughout this section, and only $\hbar$ will vary. For a given $\hbar$, the harmonic oscillator basis states define a grid in the action space (see Fig. 2). The points on the grid enclosed by the billiard are the basis states to be used in the quantum billiard. Of course, the smaller $\hbar$ is, the larger the quantum matrix.

The classical dynamics of both circle and square billiards [Fig. 2(a) and (b)] is integrable while the Bunimovich stadium [Fig. 2(c)] is chaotic. Figures 3–5 show the respective nearest neighbour distribution (NND) for different values of $\hbar$. The spectra for the circle and square action billiards follow a Poisson distribution while the stadium has a GOE type NND distribution of random matrix theory [8]. Once this general feature has been

established, we proceed to a finer study of the spectral properties of the Bunimovich stadium in connection with classical periodic orbits.

According to equation (3.3), in the semiclassical limit the oscillatory part of the level density is given by a sum over all periodic orbits with energy E. Smoothing the level density with Gaussians of width λ cuts off the contribution of orbits with periods greater than $\tau = \hbar/\lambda$. Therefore, controlling λ helps select only the shortest periodic orbits in n_{osc}. The smoothed density of states is then defined by

$$\tilde{n}_\lambda(E) = (2\pi\lambda^2)^{-1/2} \int \sum_n \delta(E' - E_n) \mathrm{e}^{-(E-E')^2/2\lambda^2} \mathrm{d}E' = \frac{1}{\lambda\sqrt{2\pi}} \sum_n \mathrm{e}^{-(E-E_n)^2/2\lambda^2}. \quad (4.1)$$

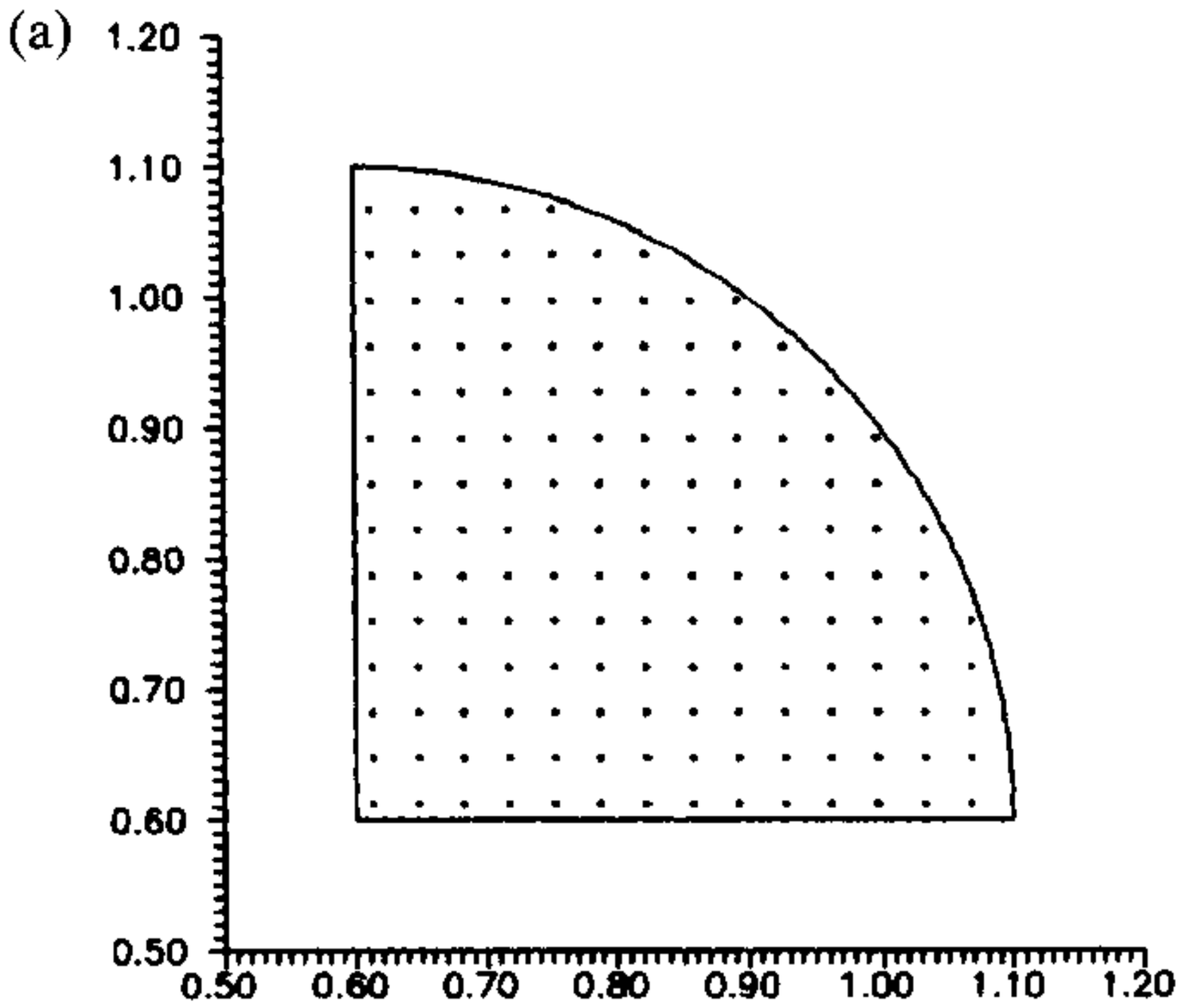

Fig. 2(a). Caption on p.383.

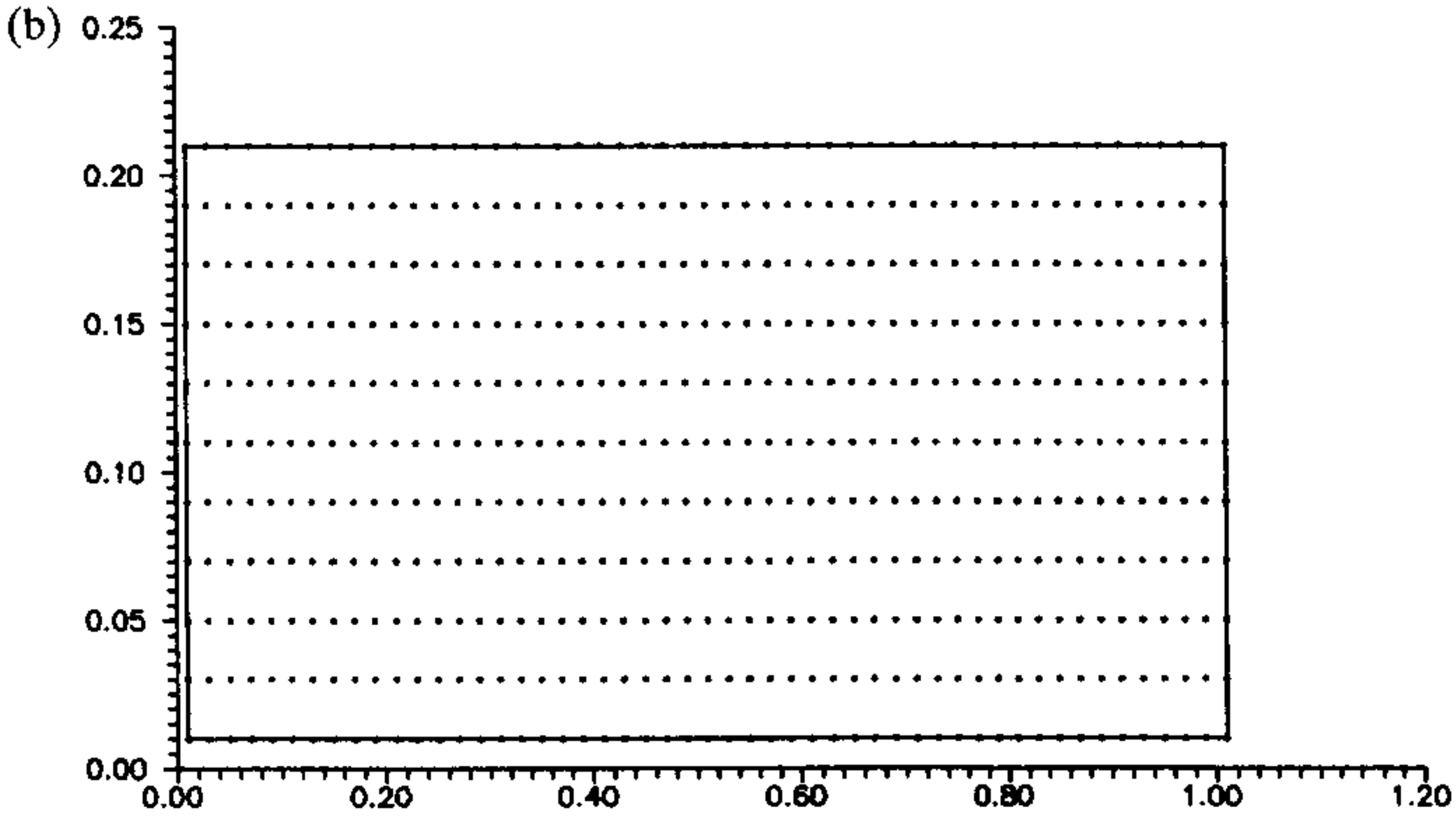

Fig. 2(b). Caption on p.383.

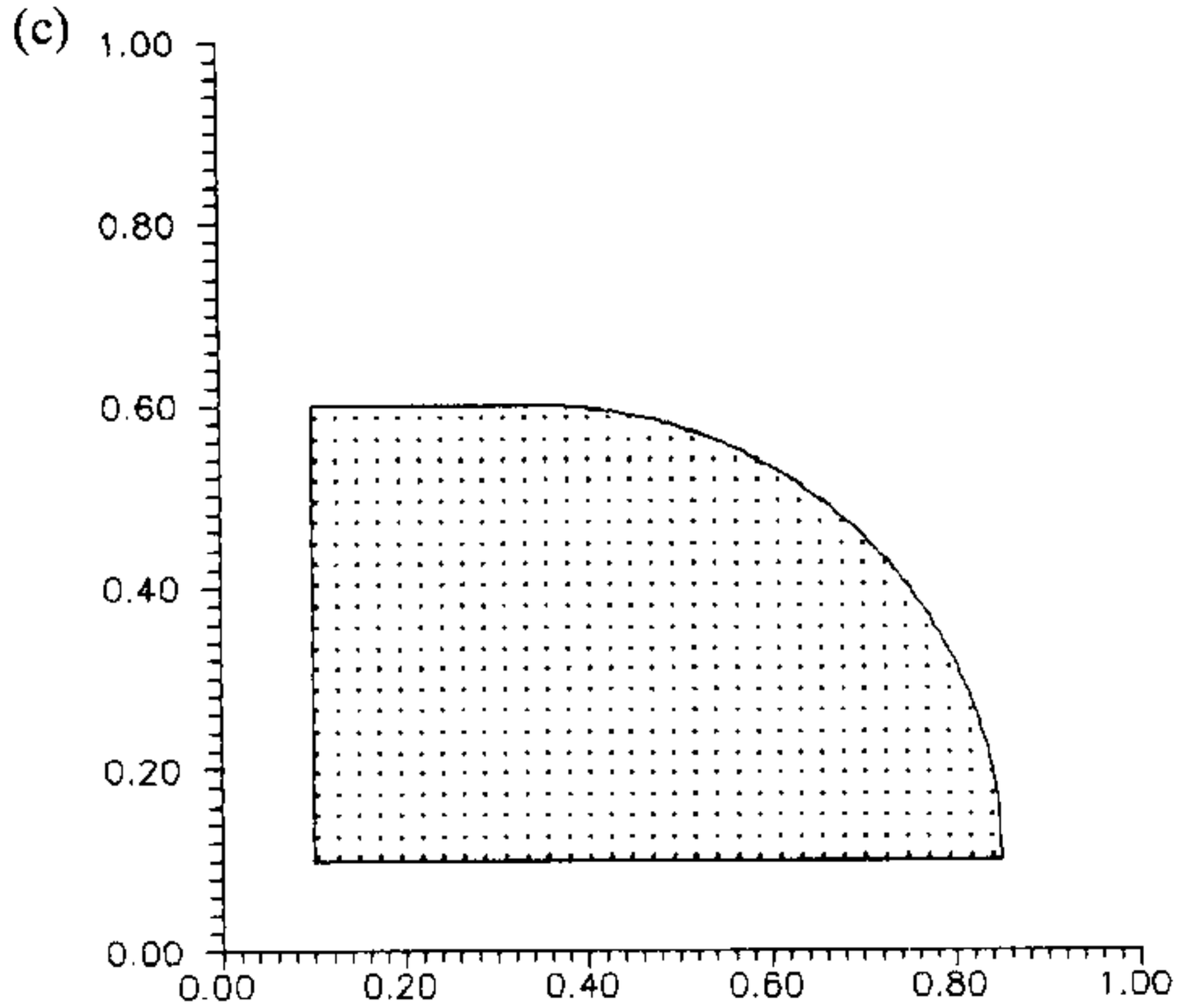

Fig. 2. Billiard enclosures for (a) quarter-circle, (b) rectangle and (c) quarter-stadium. The grid points indicate the harmonic oscillator states entering in the quantum matrix.

It is important at this point to discuss the numerical calculation of the Weyl term. One could naively expect that n_{Weyl} should be obtained as $\tilde{n}(E)$ in the limit of very large width λ. Notice however that the quantum spectrum is limited to the interval $[-2, 2]$ and that any Gaussian smoothing will tend to zero near the borders, since the spectrum terminates there. The exact calculation equation (3.9), on the other hand, gives a finite value for n_{Weyl} (± 2). Therefore, this numerical procedure will introduce errors near $E = \pm 2$ in a region of size λ. Then, the larger λ the worst the result. It must be noticed, however, that this is not a contradiction: in the strict semiclassical limit, where the number of levels per energy interval goes to infinity, any λ can be considered very large. Therefore, the regions where the numerical calculation of n_{Weyl} is bad vanish.

In practical situations, where the number of energy levels is finite, the Weyl term can still be computed using the combination of two ingredients: periodically repeated spectrum and self-consistency. That is, the original spectrum contained in the interval $[-2, 2]$ is periodically repeated through the energy axis to avoid the tendency of getting zero n_{Weyl} at $E = \pm 2$. This, however, is not enough as can be seen in Figs 6 and 7 where the spectrum has been repeated periodically in the interval $[-4, 4]$. It is seen that good results at the border $E = \pm 2$ can be obtained only at the expense of a flat maximum at $E = 0$, instead of the divergence of the exact result. This is because of the very different values assumed by the local density of states. A given λ may be very large when used near $E = 0$ but still small for E near ± 2. This is why self-consistency is needed: once $\tilde{n}(E)$ has been calculated, a local width is computed as $\Delta(E) = 1/\tilde{n}(E)$ and the calculation is re-started. As this process is iterated the smoothed Weyl density gets closer to the exact calculations, as shown in Fig. 8. We shall call $\bar{n}_{\text{Weyl}}(E)$ the numerical self-consistent calculation of the Weyl term. For any Gaussian width λ we define the oscillatory density

$$\bar{n}_{\text{osc}}(E) = \tilde{n}_{\lambda}(E) - \bar{n}_{\text{Weyl}}(E). \tag{4.2}$$

Before showing the results for $\bar{n}_{\text{osc}}$ let us first study the behaviour of the simplest periodic orbit families in the stadium. The shortest orbits are the so called 'bouncing ball'

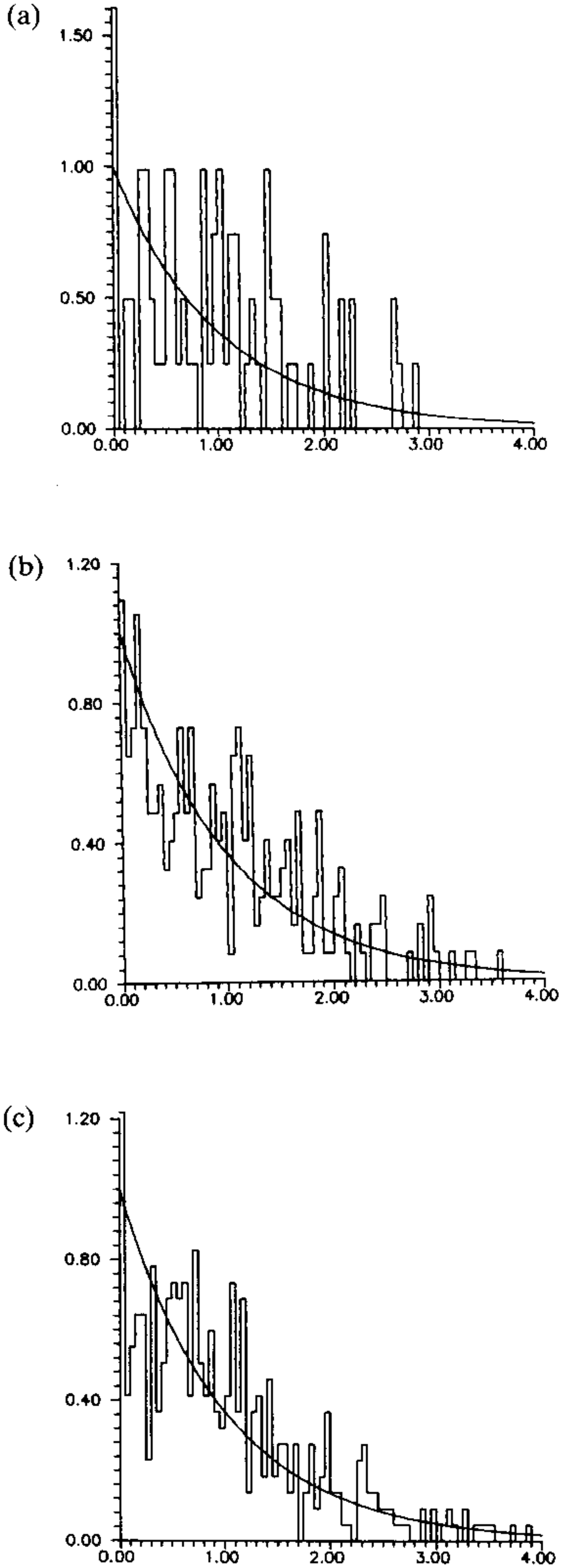

Fig. 3. Nearest neighbour distribution for the quarter circle for different values of $\hbar$ and matrix dimension N. In (a) $\hbar = 0.035$, $N = 162$; in (b) $\hbar = 0.020$, $N = 494$ and in (c) $\hbar = 0.015$, $N = 870$.

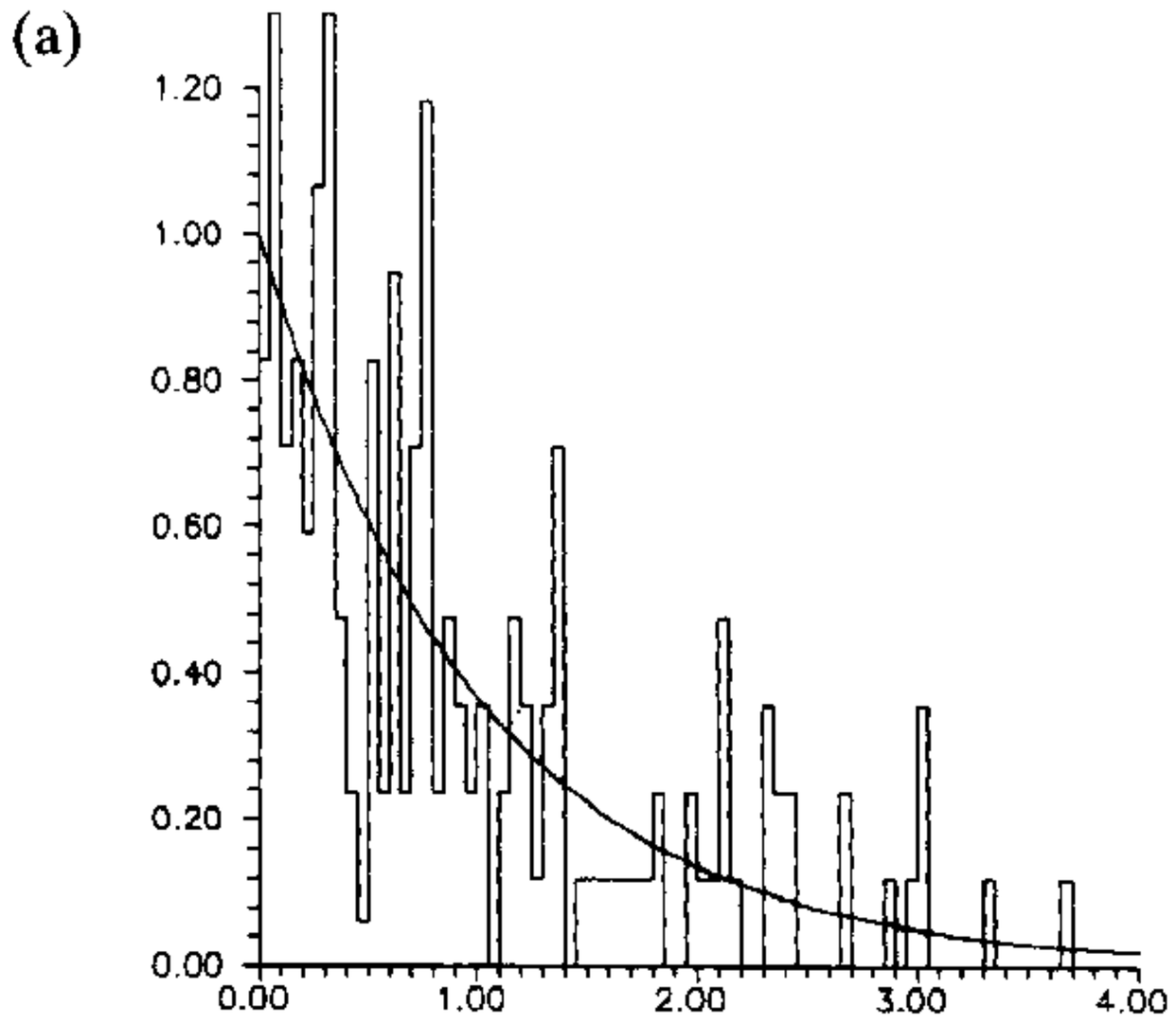

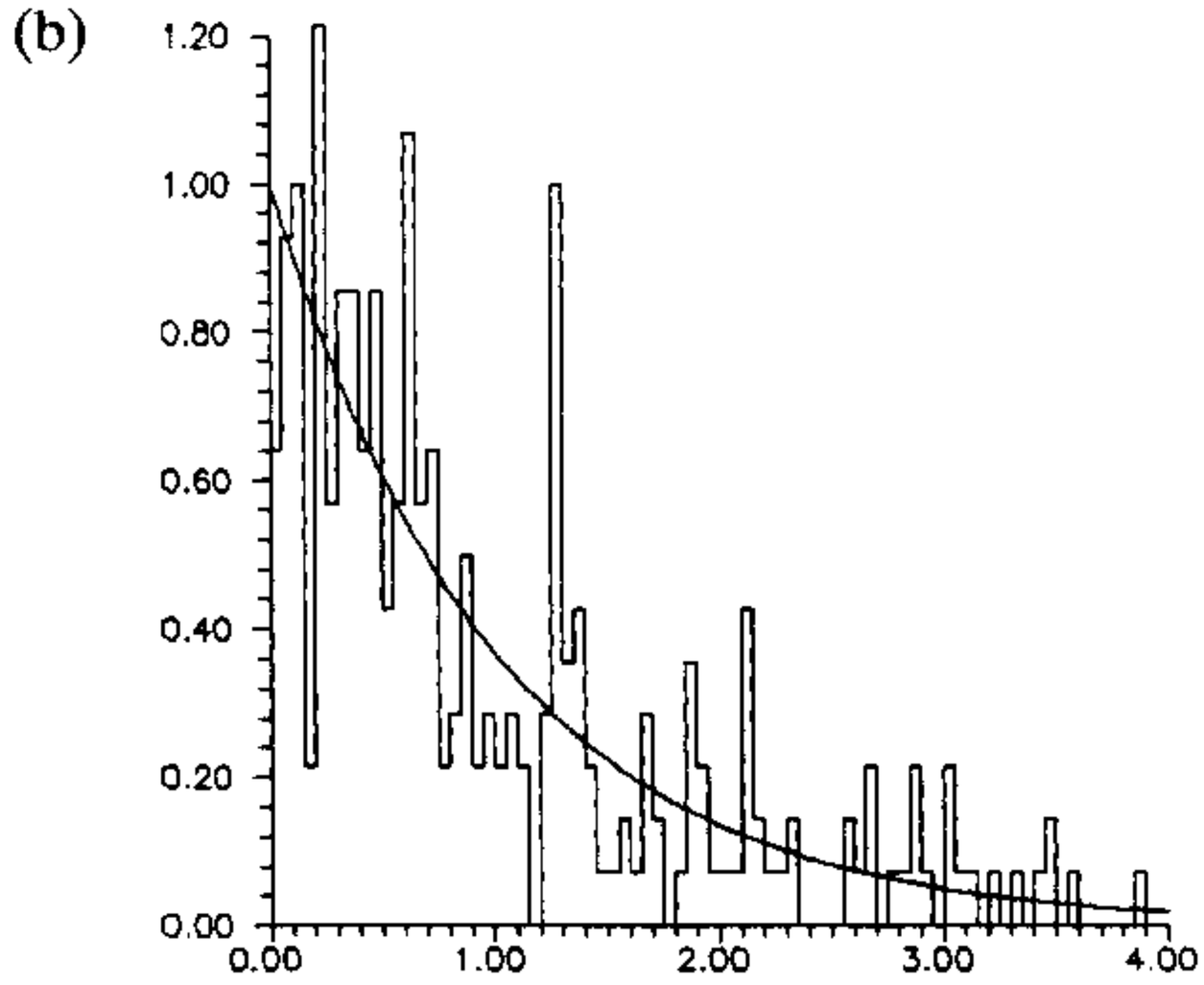

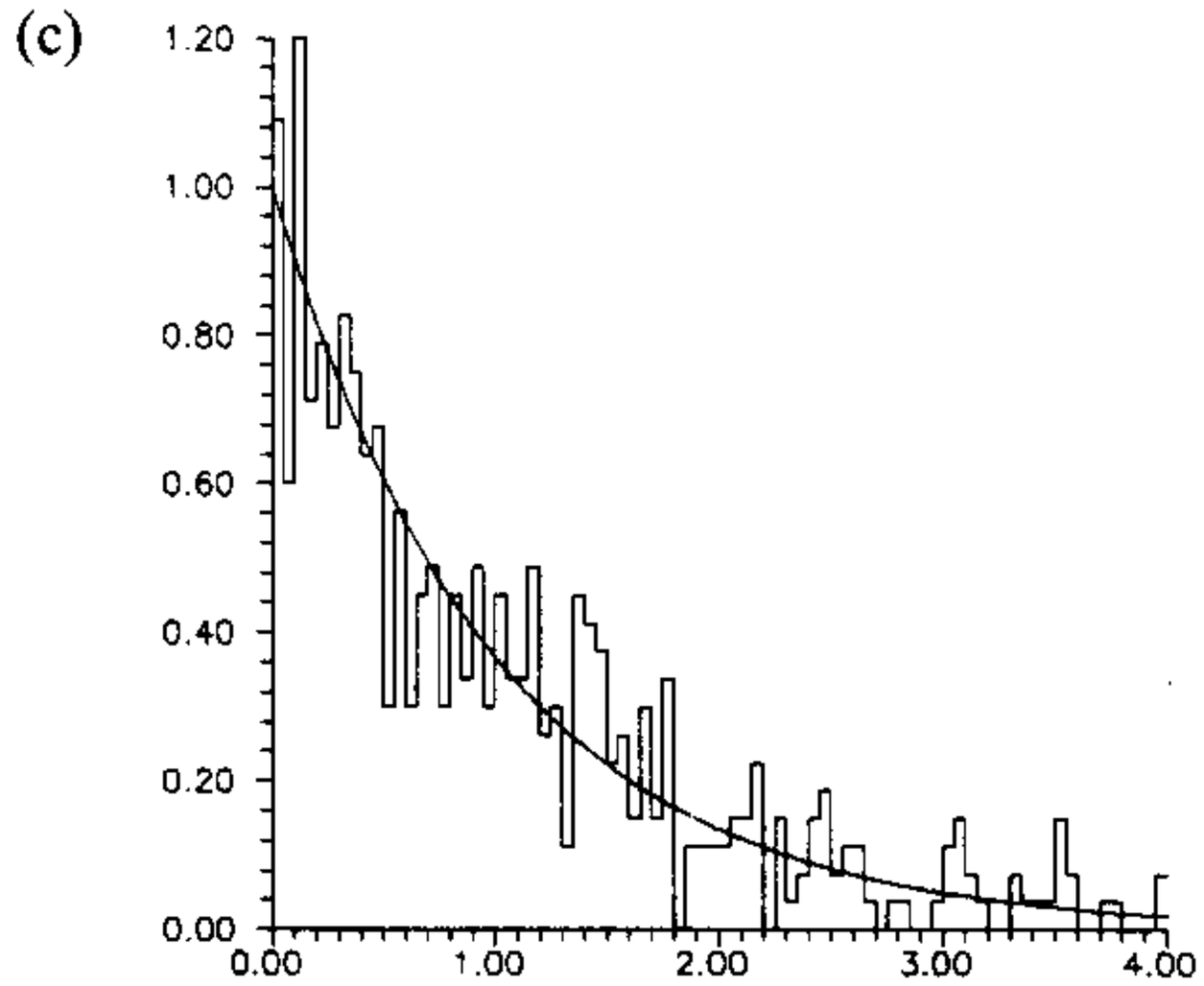

Fig. 4. Nearest neighbour distribution for the rectangle for different values of $\hbar$ and matrix dimension N. In (a) $\hbar = 1/25$, $N = 156$; in (b) $\hbar = 1/50$, $N = 561$, in (c) $\hbar = 1/70$, $N = 1065$.

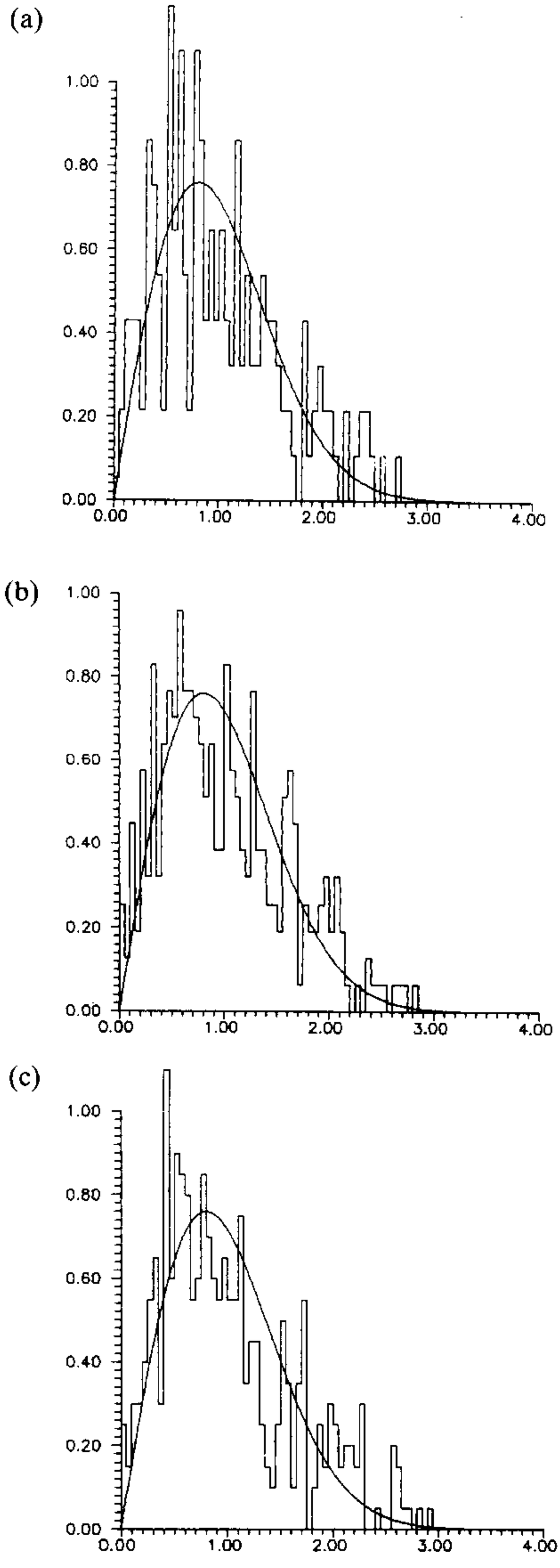

Fig. 5. Nearest neighbour distribution for the quarter-stadium for different values of $\hbar$ and matrix dimension N. In (a) $\hbar = 0.03$, $N = 372$; in (b) $\hbar = 0.023$, $N = 627$ and in (c) $\hbar = 0.02$, $N = 801$.

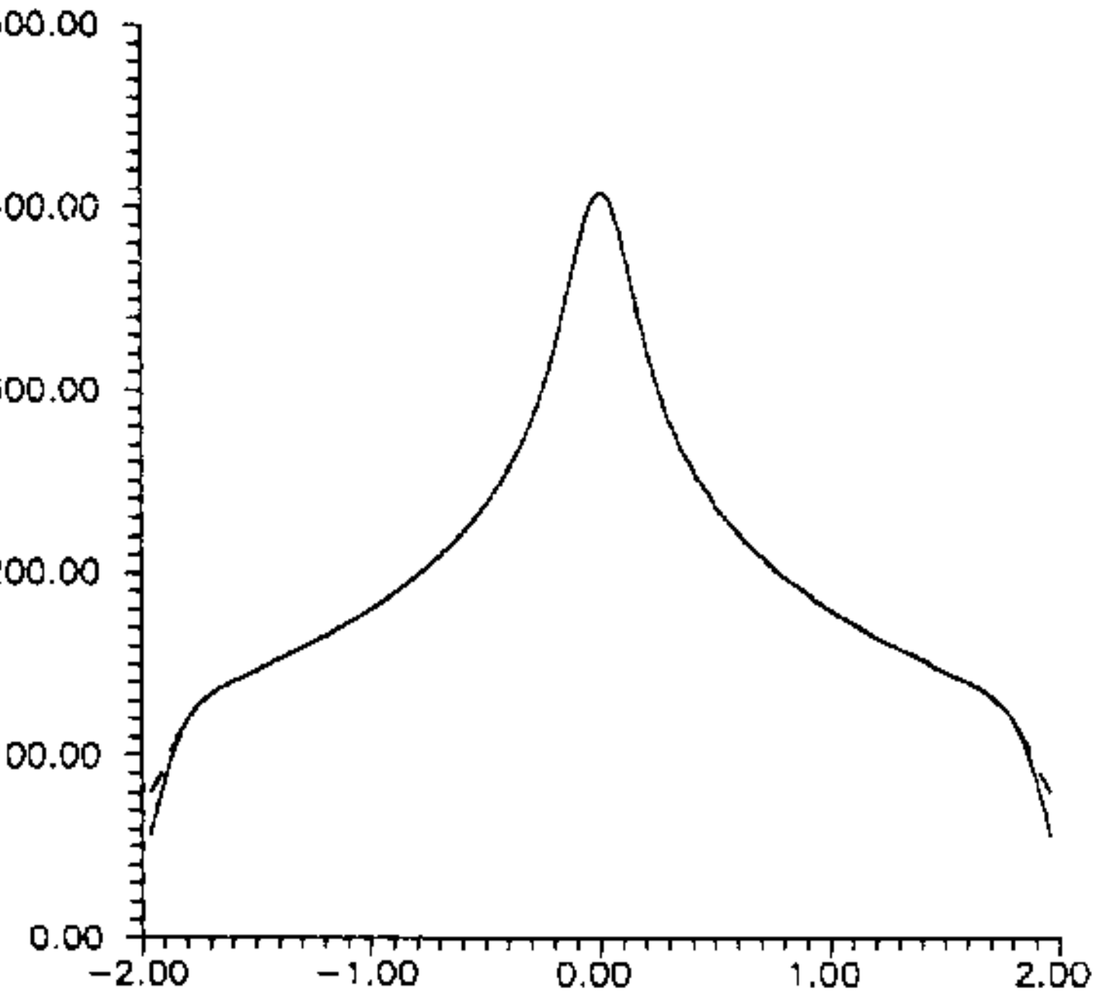

Fig. 6. Weyl density of states for the quarter-stadium for $\hbar = 0.02$ and energy smoothing $\lambda = 0.1$. The broken curve was obtained with a periodically doubled spectrum and the continuous curve is the usual calculation.

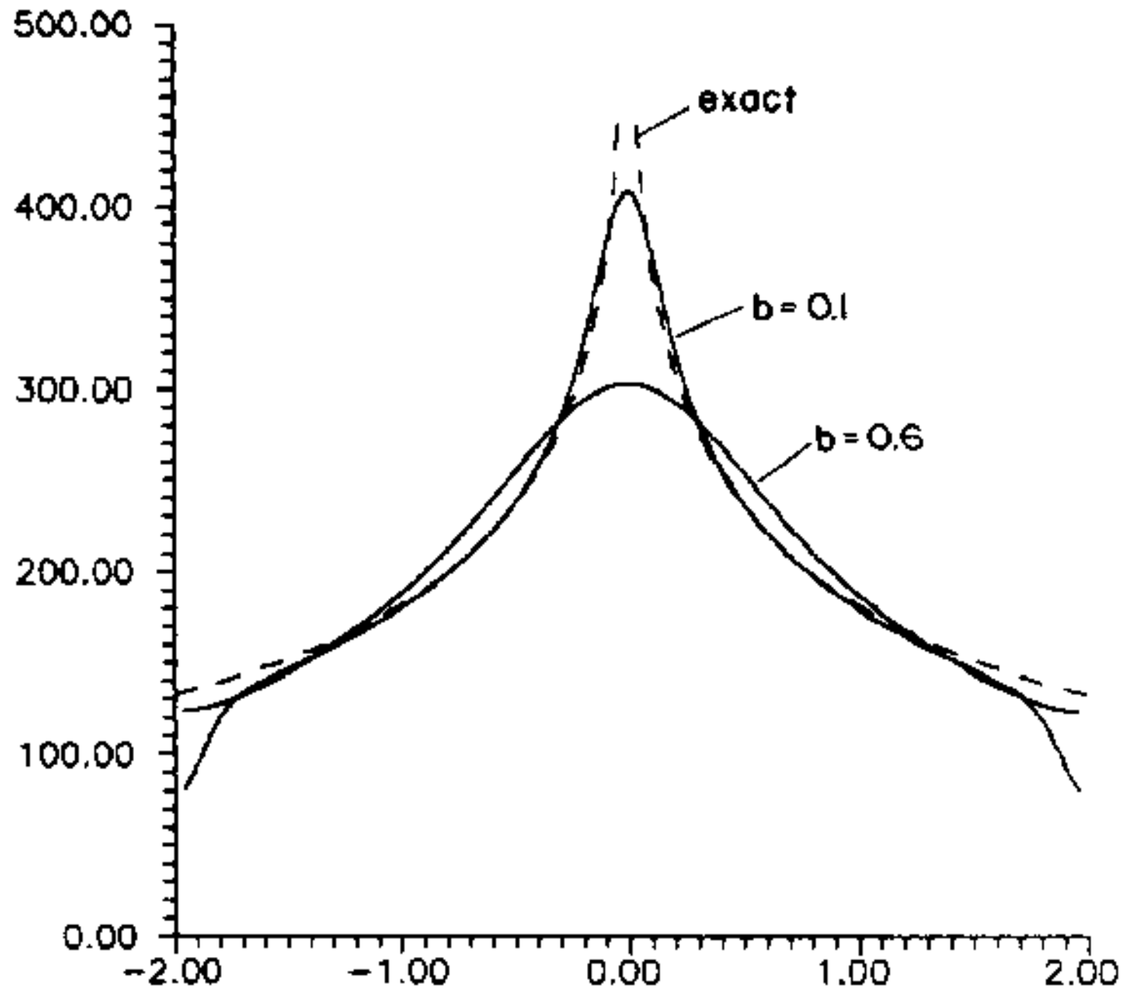

Fig. 7. Weyl density of states for $\hbar = 0.02$ with the periodically doubled spectrum and different smoothings: $\lambda = 0.1$ and $\lambda = 0.6$. The broken curve is the exact result.

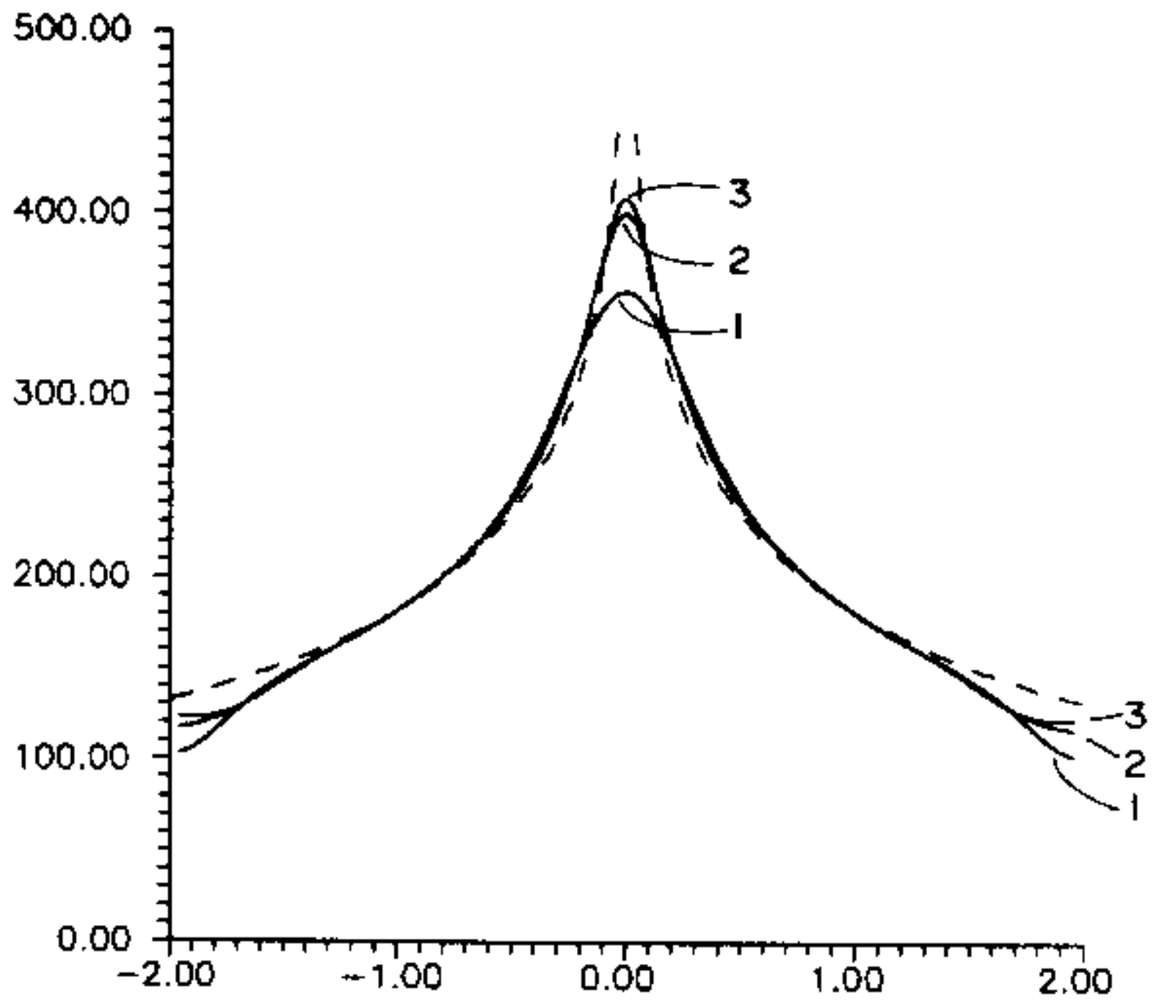

Fig. 8. Self-consistent calculation of the Weyl density of states for $\hbar = 0.02$ with the periodically doubled spectrum. The local smoothing was taken as 40 times the local mean spacing. The broken curve is the exact result and the labels show the number of iterations for each calculation.

given by

$$I_1 = I_{10} = \text{constant}$$
$$I_2 = t \sin \theta_{20}$$
$$\theta_1 = 0 \text{ or } \pi$$
$$\theta_2 = \pm\theta_{20}$$
$$E = -1 - \cos\theta_{20} \text{ or } E = 1 - \cos\theta_{20}.$$

The period of such orbits can be easily calculated in terms of E and R, the radius of the semi-circles forming the stadium (see Fig. 2). For $E > 0$ ($\theta_1 = \pi$) it gives

$$T = \frac{2R}{\sqrt{(2E - E^2)}} \tag{4.3}$$

with a similar expression for $E > 0$, as displayed in Fig. 9.

Other periodic orbits present similar $E \times T$ plots, with the period depending strongly on the energy and with $\partial T/\partial E\ (E = 0) = \infty$. Therefore, the best place to look for scars of periodic orbits is in the vicinity of $E = 1$ or $E = -1$. Besides, concentrating the calculation in these regions avoids the numerical problems with the Weyl term occuring near $E = 0$ and $E = \pm 2$.

Figures 10–12 show plots of $n_\lambda(E)$, $\bar{n}_{\text{osc}}(E)$ and the Fourier transform of $\bar{n}_{\text{osc}}(E)$ for different values of λ (0.03, 0.02 and 0.01 respectively). The Fourier analysis of $\bar{n}_{\text{osc}}(E)$ is restricted to the energy interval [0.5, 1.5]. Figure 10 shows a single peak at $T = 1$, corresponding to the shortest orbit, the bouncing ball [notice that $R = 0.5$ in equation (4.3)]. As λ diminishes new orbits start to contribute to $\bar{n}_{\text{osc}}$. Figure 11 shows a second peak at $t = 1.75$, corresponding to the periodic orbit running horizontally above the lower boundary of the quarter-billiard (this is the second shortest orbit). Finally Fig. 11(c) shows several other peaks: $T = 2$ represents two repetitions of the bouncing ball; $T = 3$ counts three repetitions of the bouncing ball plus 2 repetitions of the horizontal orbit; between $T = 2$ and $T = 3$ several other orbits (more complicated) can also be distinguished (see for instance [9]).

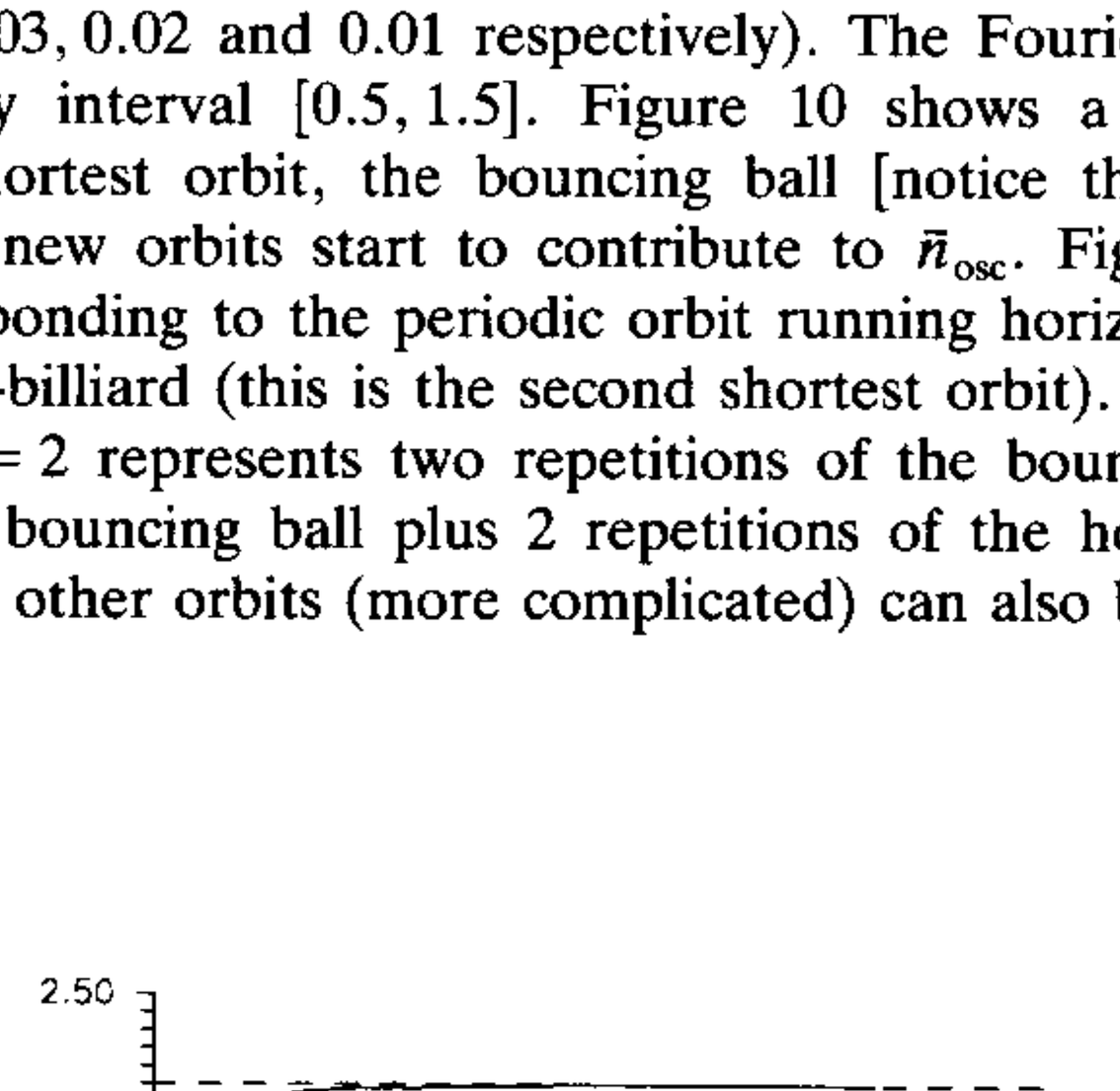

Fig. 9. Energy vs period plot for the horizontal orbit.

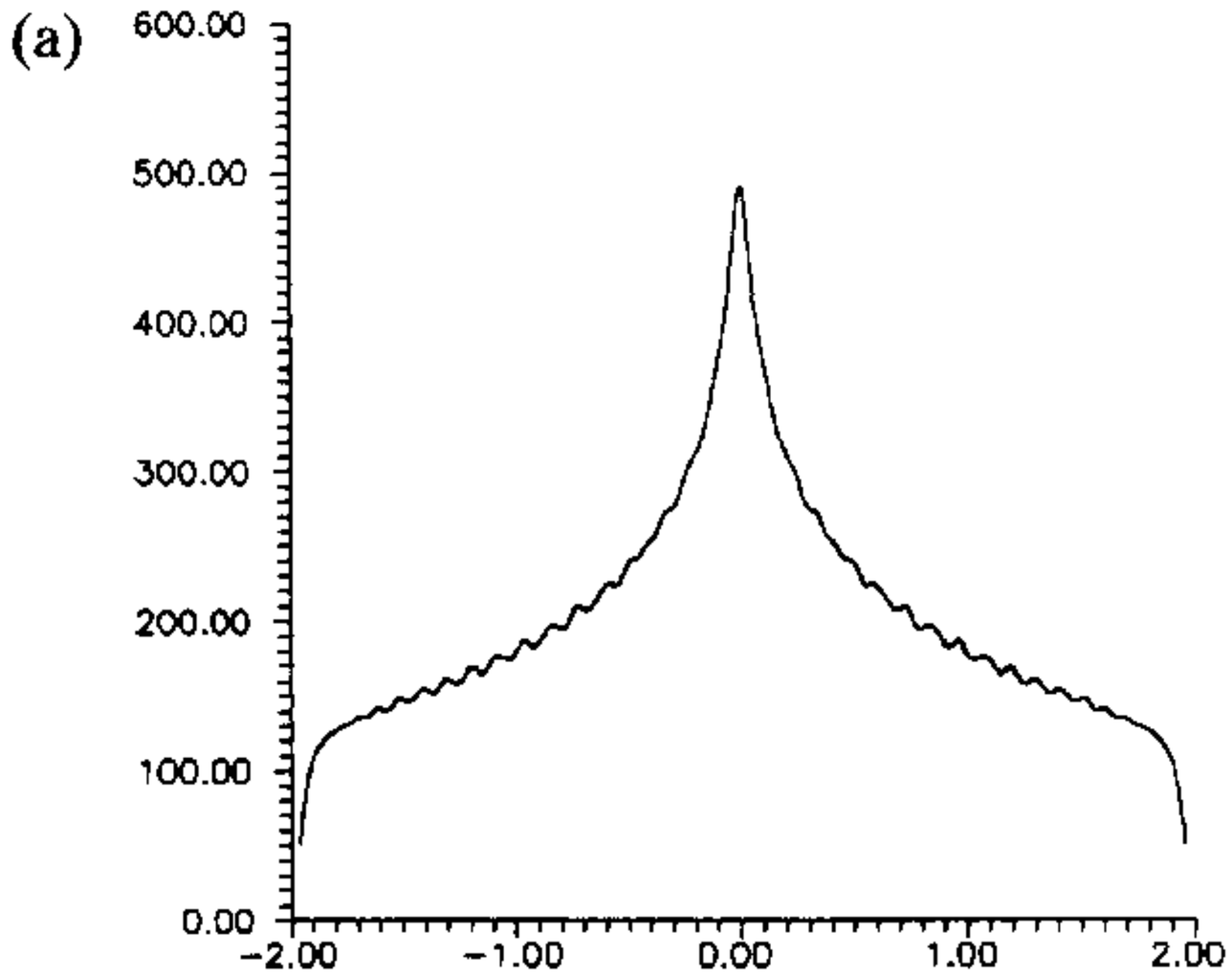

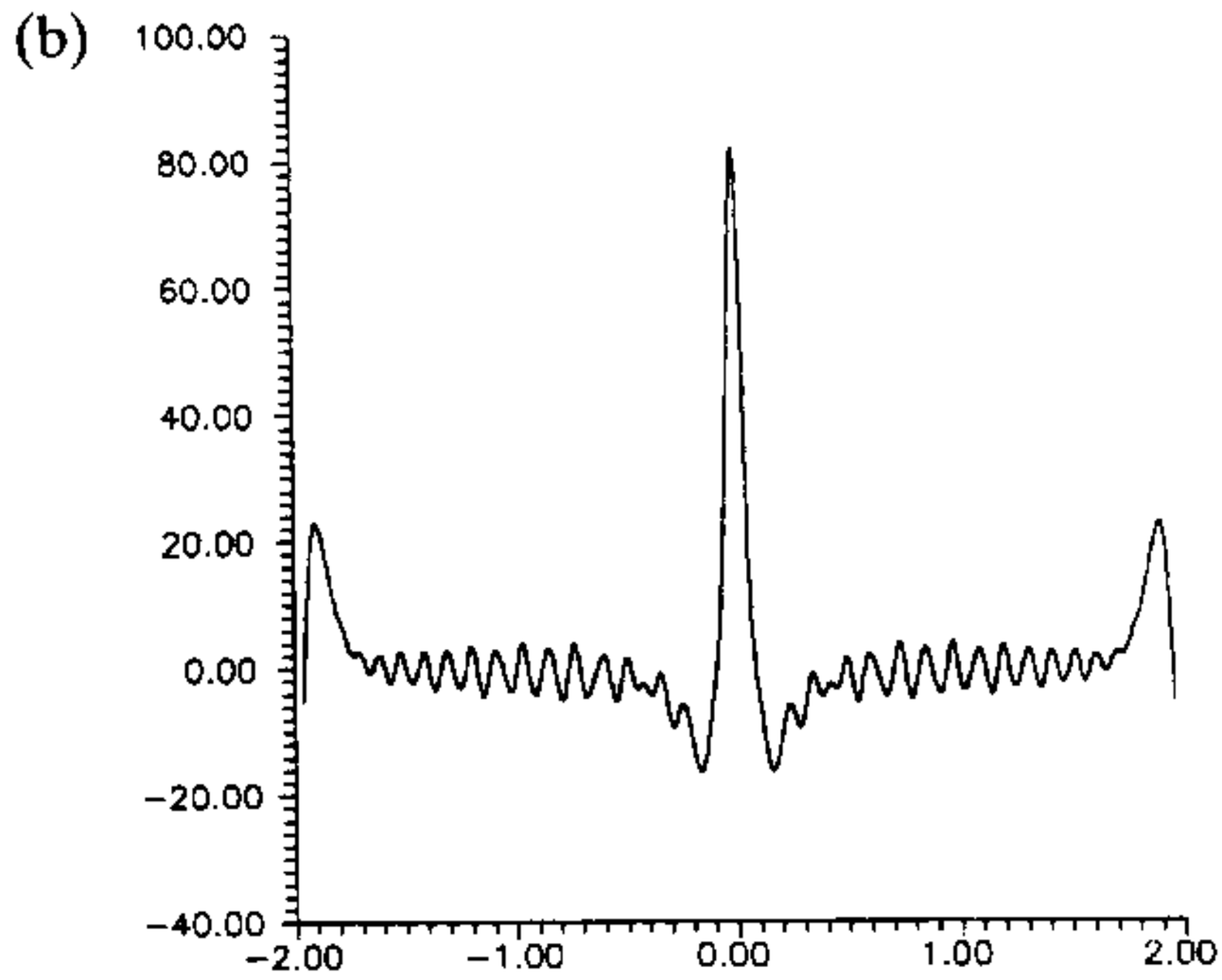

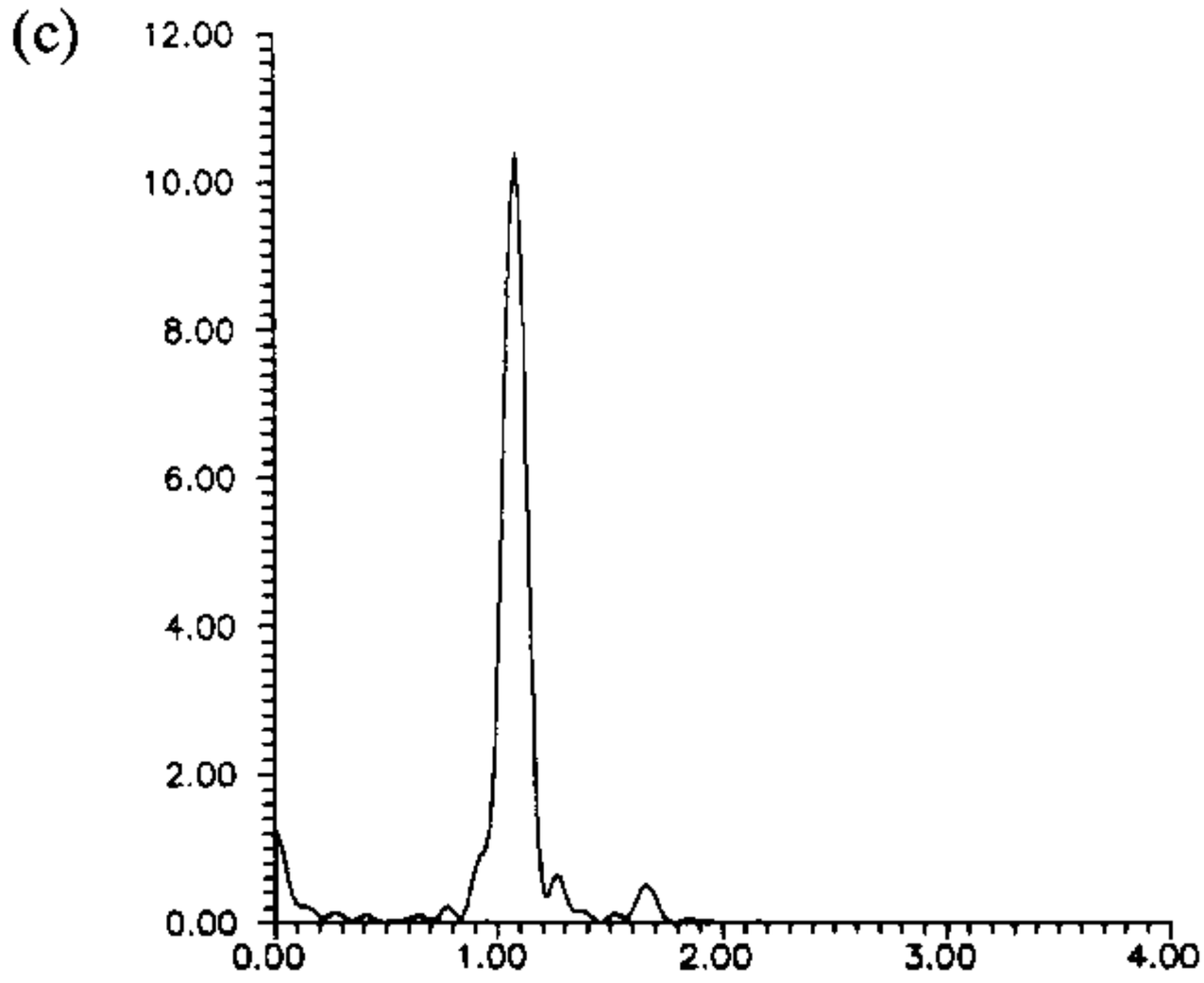

Fig. 10. (a) Smoothed density of states for $\hbar = 0.02$ and $\lambda = 0.03$. (b) $\bar{n}_{\mathrm{osc}}$ for the same parameters. (c) Fourier spectrum of $\bar{n}_{\mathrm{osc}}$.

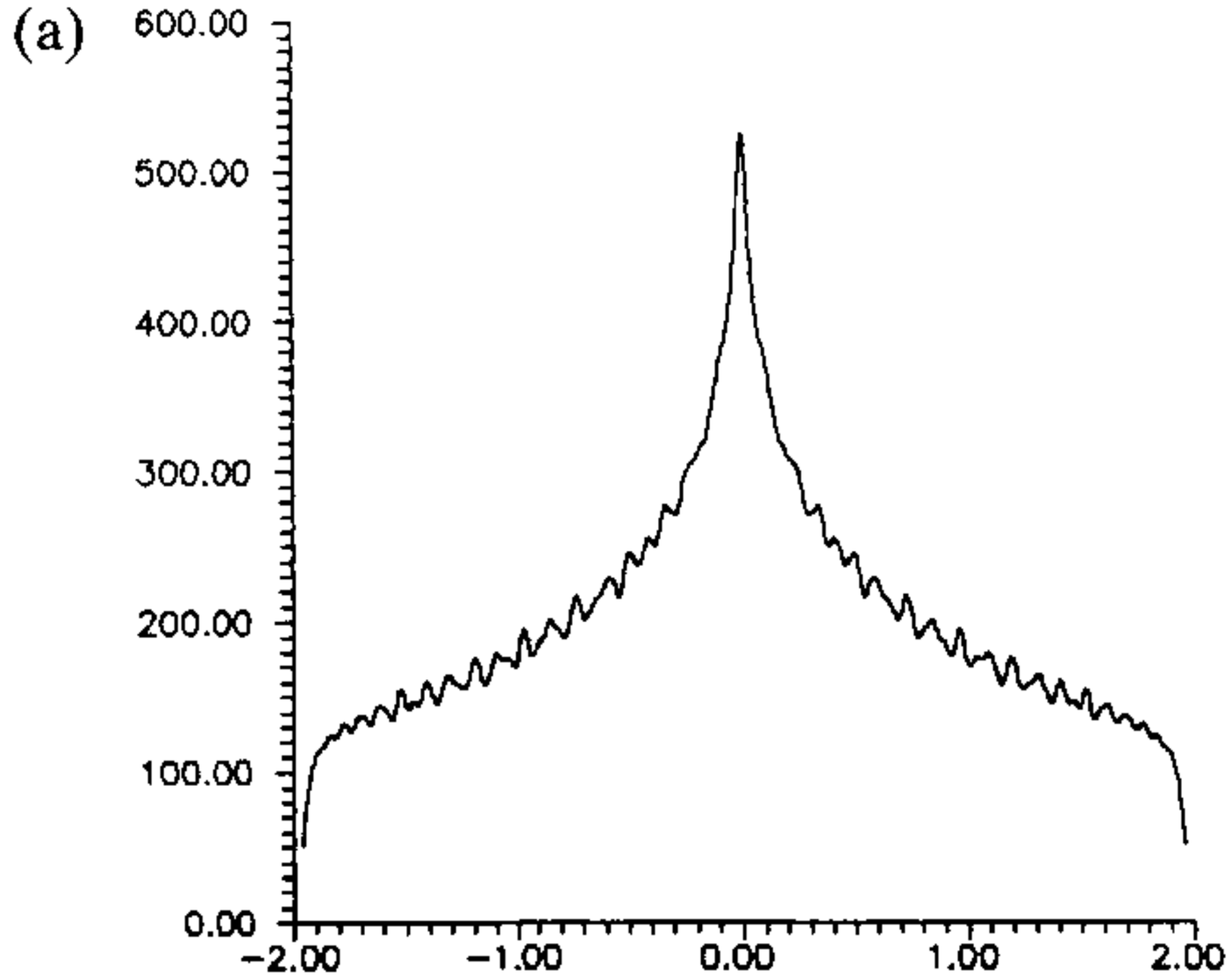

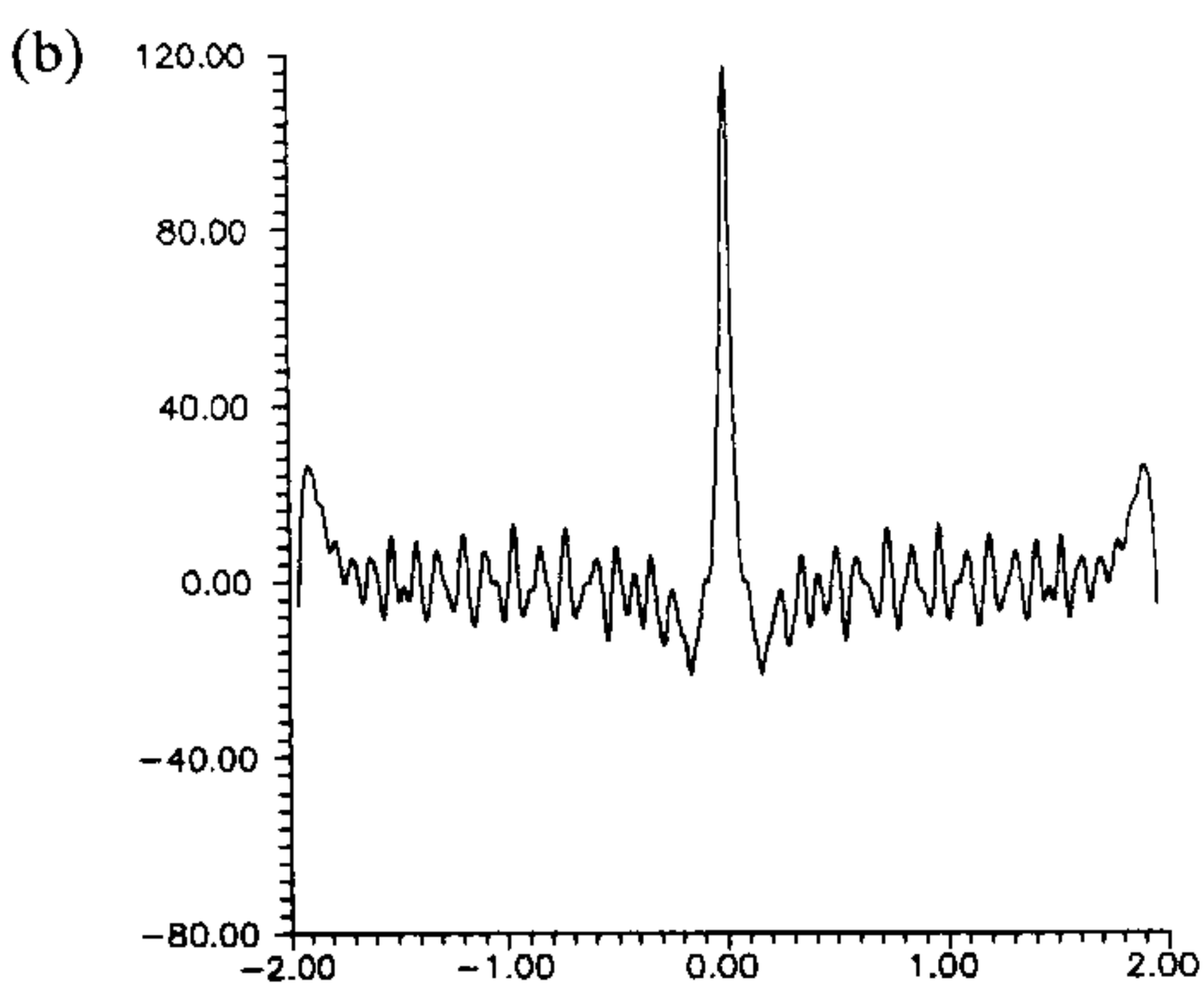

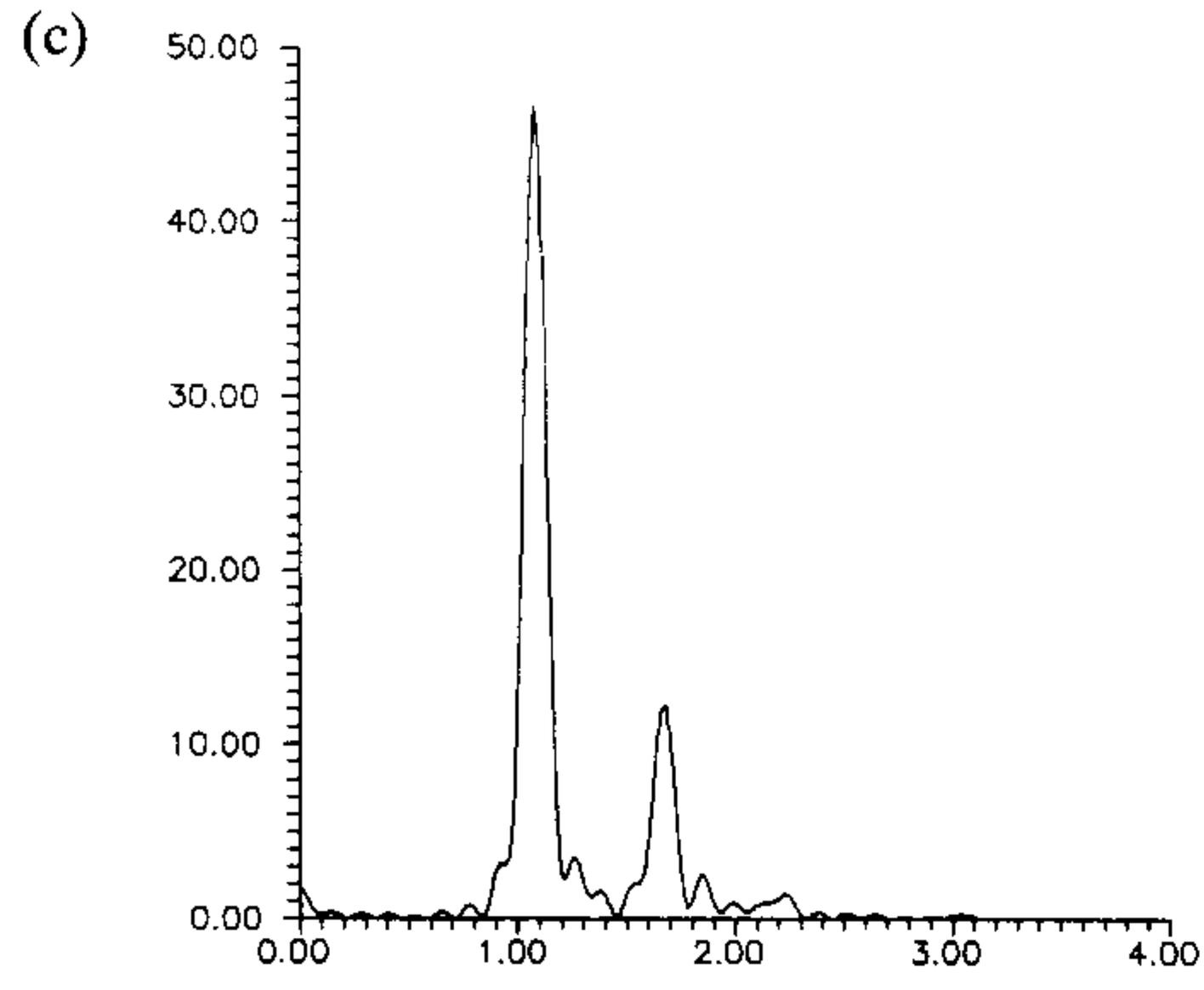

Fig. 11. The same as in Fig. 10 with $\lambda = 0.02$.

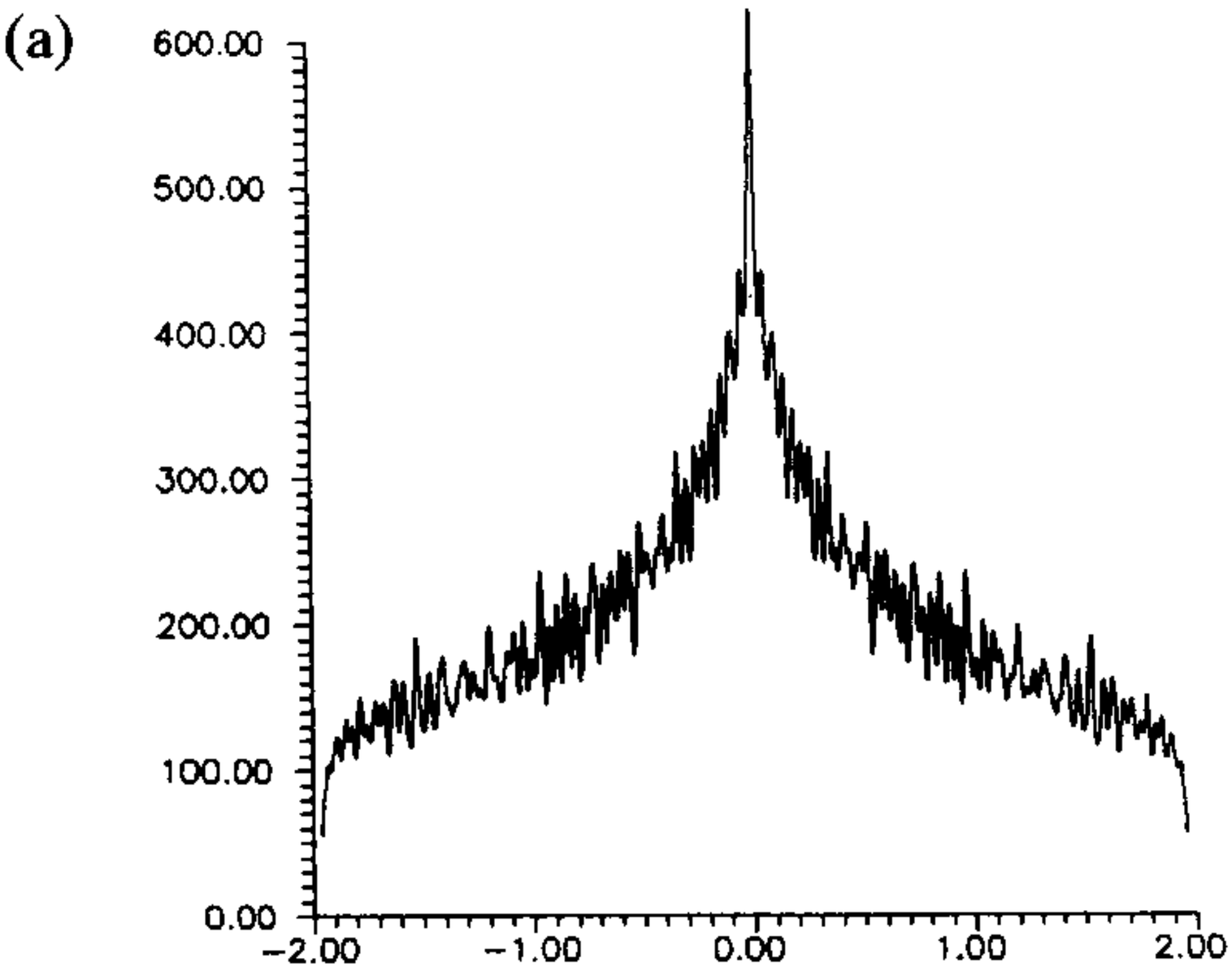

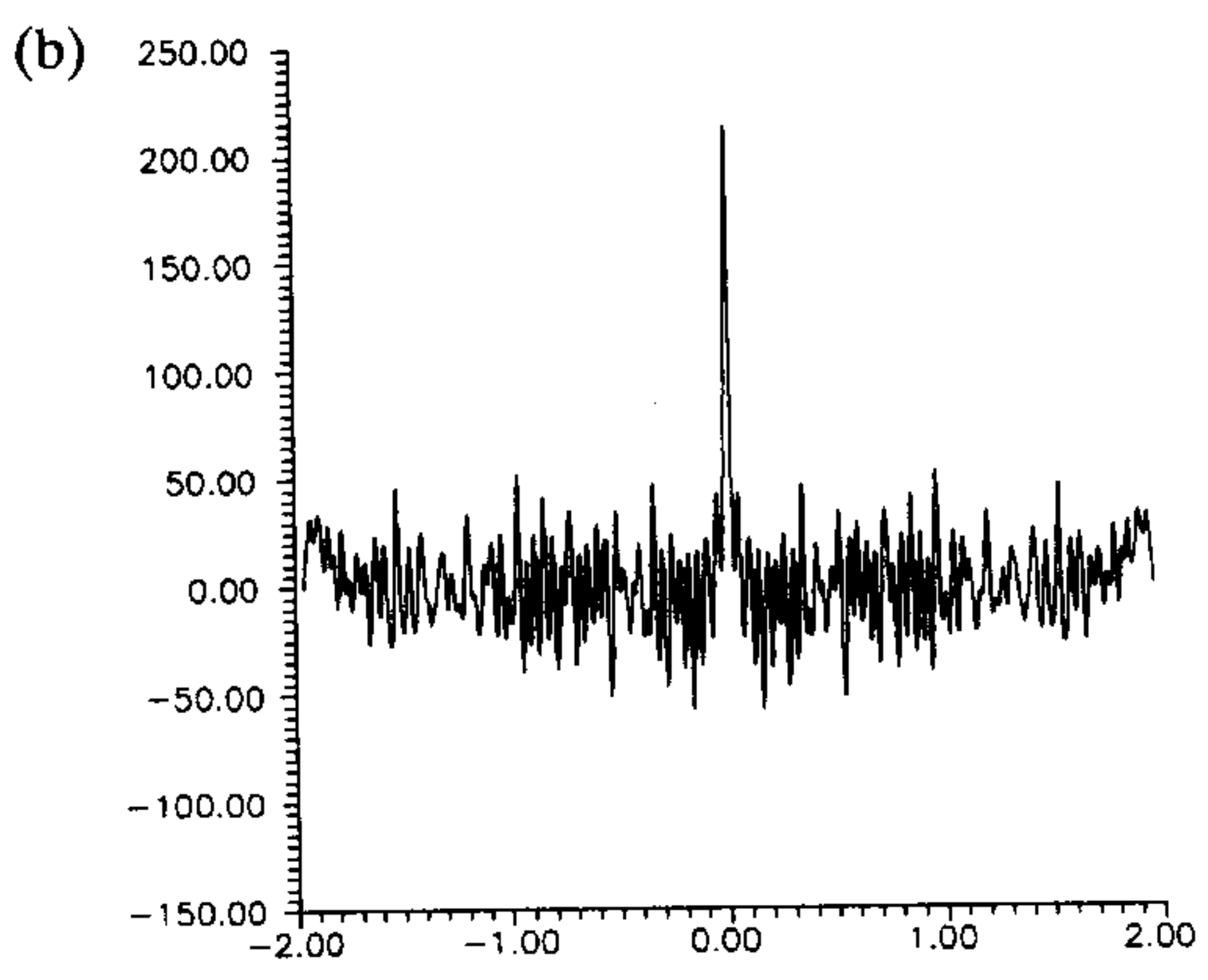

Fig. 12. The same as in Fig. 10 with $\lambda = 0.01$.

5. CONCLUSION

The results of the previous sections show that action billiards are very good models for the study of quantum chaos. Indeed, they can be chosen to present dynamics ranging from integrable to completely chaotic, always with finite quantum analogues. We have checked that, for the case of the Bunimovich billiard, the results of the usual semiclassical theory of periodic orbits apply exactly as in common billiards. It is important to emphasize that the present quantum system is radically different from the usual quantized stadium. The verification of the validity of the GOE nature of the spectral statistics and the contribution of individual periodic orbits to its fluctuations provides a dramatic confirmation of how these features are exclusively determined by the underlying classical motion.

Acknowledgements—This work was partially supported by FAPESP, CNPq and FINEP.

REFERENCES

1. J. H. Hannay and M. V. Berry, *Physica* **1D**, 267 (1980).
2. N. Balazs and A. Voros, *Ann. Phys.* **190**, 1 (1989).
3. P. Leboeuf and M. Saraceno, *J. Phys. A Math. Gen.* **23**, 1745 (1990).
4. M. A. M. de Aguiar and A. M. Ozorio de Almeida, *Nonlinearity* (1991) (to appear).
5. M. A. M. de Aguiar, *Phys. Lett.* (to appear).
6. M. C. Gutzwiller, *J. Math. Phys.* **12**, 343 (1971).
7. I. Gradshteyn and I. M. Ryzhik, *Table of Integrals, Series and Products*, 4th Edition, p. 246. Academic Press, New York, (1965).
8. O. Bohigas and M. J. Giannoni, Chaotic motion and random matrix theory, in *Mathmatical and Computational Methods in Nuclear Physics*, edited by J. S. Dehesa, J. M. G. Gomez and A. Polls, in *Lecture Notes in Physics*, Vol. 208, p. 1. Springer, Berlin (1984).
9. E. G. Bogomolny, *Physica* **31D**, 169 (1988).